CONTROL OF A WHEELED ROBOT FOLLOWING A CURVILINEAR PATH

Alexander V. Pesterev
Institute of Control Sciences RAS
and Javad GNSS
Moscow, Russia
A.Pesterev@javad.com

Lev B. Rapoport
Institute of Control Sciences RAS
and Javad GNSS
Moscow, Russia
L.Rapoport@javad.com

Ruslan F.Gilimyanov
Institute of Control Sciences RAS
and Javad GNSS
Moscow, Russia
R.Gilimyanov@javad.com

Abstract

A control synthesis problem for planar motion of a wheeled robot is considered. The control goal is to bring the robot to a given path and to stabilize motion of a certain target point along it. The trajectory is assumed to be an arbitrary smooth curve with bounded curvature. A simple actuator is introduced into the vehicle model, and the rate of angular rotation of the steering wheels is taken as the control, which is subject to two-sided constraints. In addition, because of phase constraints, the system under consideration is hybrid: at different stages of its motion, it is governed by different systems of differential equations. A control law is synthesized for an arbitrary target path. Qualitative analysis of the straight line case is given. Results of numerical experiments are presented.

Key words

Wheeled robots, feedback linearization, phase constraints

1 Introduction

There are many applications (e.g., in road construction or agriculture) where a vehicle is to be automatically driven along some path with high level of accuracy. This can be achieved if the robot is equipped with satellite and inertial navigation tools, see [Cordesses, Cariou, and Berducat, 2000], [Thuilot et al., 2002], and [Rapoport et al., 2006].

Control problems for mobile robots are considered in many papers (e.g., [Cordesses, Cariou, and Berducat, 2000], [Thuilot et al., 2002], [Samson, 1995], [Kolmanovsky and McClamroch, 1995], [Guldner and Utkin, 1994], and references therein). Control laws are designed that stabilize motion along a straight line or motion towards a given point in the plane. The control can be either continuous ([Cordesses, Cariou, and Berducat, 2000], [Thuilot et al., 2002]) or discontinuous ([Guldner and Utkin, 1994], [Kolmanovsky and McClamroch, 1995]). Here, we consider the control design problem with regard to the actuator dynamics and boundedness of controls.

The control goal is to bring the robot to a given path and to stabilize motion of a certain target point along it. The path is assumed to be an arbitrary smooth curve with bounded curvature. A control law that brings the vehicle in the vicinity of the target path from an arbitrary initial position and guarantees a specified rate of exponential convergence in some neighborhood of the path is constructed. Qualitative analysis of the case of a straight target path is given, and a numerical example is considered.

2 Problem Statement

The goal of the control is to place the robot (vehicle) in the desired trajectory on the plane and stabilize its motion along the target curve. The trajectory is assumed to be an arbitrary smooth curve satisfying some additional constraints on its curvature to make it feasible for the given vehicle. We consider the case of a parameterized representation, and, for the parameter, take the curve length s (natural representation). The target trajectory (path) is described by a pair of functions $(X(s), Y(s))$, where $X(s)$ and $Y(s)$ are x- and y-coordinates of the current point on the curve. The functions $X(s)$ and $Y(s)$ are assumed to be three times differentiable and $k(s)$ denotes the curvature of the trajectory given by

$$k(s) = \frac{X_s'' Y_s' - X_s' Y_s''}{[(X_s')^2 + (Y_s')^2]^{3/2}}, \qquad (1)$$

where the prime denotes differentiation with respect to s. The curvature is assumed to be bounded, $|k(s)| \le k_{max}$, where k_{max} is determined by the minimum turning radius of the vehicle, $k_{max} = 1/R_{min}$.

To take into account that the angle of the steering wheels cannot be changed instantaneously, we introduce a simple actuator in the vehicle model and take

the rate of angular rotation of the steering wheels for the control.

3 Kinematic Scheme and Governing Equations

The model of a wheeled robot is represented in Fig. 1 (see [Rapoport, 2006] for detail). The target point C is located at the middle of the rear axle of the platform and is denoted by $X_c = (x_c, y_c)^{\mathrm{T}}$. For the planar case, the orientation is defined by angle θ between the center line of the platform and the x-axis. Every point X_p of the platform has its own instantaneous velocity vector v. Vectors, orthogonal to the instant velocities intersect a single point X_0 known as instantaneous center of velocity.

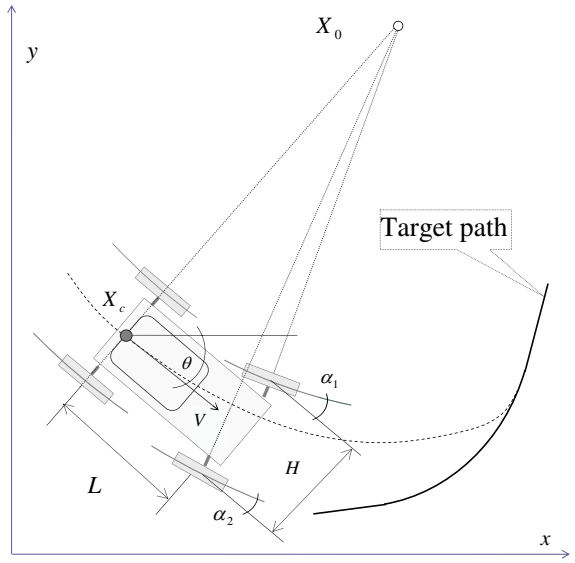

Figure 1. The kinematic scheme of the wheeled robot.

Let $\dot\theta$ be an instantaneous angular rate of the rotation of the platform. Then, the following relationship holds:

$$|\dot\theta| = \|v\|/\|X_p - X_0\|. \tag{2}$$

Hereinafter, $\|\cdot\|$ denotes the Eucledian vector norm. The condition that each of the wheels move without lateral slippage means that the vectors of instantaneous velocities of the axles' endpoints are collinear to the planes of the wheels; the normals to each of these vectors intersect at the point X_0.

The two rear wheels are driving and the front wheels are steering. For straight-line motion, the point X_0 is located at infinity and expression (2) yields zero angular rate. For the rear axle, the instantaneous center of velocity coincides with the instantaneous center of curvature. Particularly, for the target point the value $\|X_c - X_0\|$ is the instantaneous radius of curvature of the trajectory (dashed line in Fig. 1) circumscribed by the target point X_c. The reciprocal to the radius $1/\|X_c - X_0\|$ is the instantaneous curvature denoted by u. Let L and H be dimensions of the platform, as shown in Fig. 1. Then, the relationship between the curvature and the steering angles is given by

$$\frac{uL}{1 - uH/2} = \tan\alpha_1, \quad \frac{uL}{1 + uH/2} = \tan\alpha_2. \tag{3}$$

Positive curvature and steering angles are associated with the left (counterclockwise) turn, which is shown in Fig. 1.

It follows from (3) that α_1 and α_2 are not independent. For simplicity, instead of two angles, we introduce an "average" angle α by the equation

$$\tan\alpha = uL. \tag{4}$$

To take into account the actuator dynamics, we assume that the steering angle is controlled by specifying the angular velocity V of the driving shaft of the actuator, $\dot\alpha = V$. This kind of actuator dynamics describes, e.g., step motors often met in practice.

Finally, denoting by v_c the scalar linear velocity of the vehicle, we arrive at the following well-known model describing motion of a simple controlled vehicle with regard to the actuator dynamics:

$$\begin{aligned} \dot x_c &= v_c\cos\theta, \\ \dot y_c &= v_c\sin\theta, \\ \dot\theta &= v_c u(\alpha), \\ \dot\alpha &= V, \end{aligned} \tag{5}$$

where $u(\alpha)$ is determined by (4).

The limitations on the steering angle impose two-sided phase constraints:

$$-\bar u \le u \le \bar u \ (-\alpha_{max} \le \alpha \le \alpha_{max}), \tag{6}$$

where $\bar u = \tan\alpha_{max}/L$. This implies that, when the phase variable α (or u) reaches its upper (lower) bound, the control V must be set equal zero, whatever control strategy was applied before. After this, the system moves in the hyperplane $u = \bar u$ ($u = -\bar u$), and its motion is governed by the first three equations in (5) (the order of the system reduces by one). When the control is turned on again (clearly, the sign of V must change), the system is governed again by equations (5).

Thus, the presence of phase constraints (6) makes the system under consideration not only nonlinear, but also hybrid: at different stages of its motion, it is governed by different systems of differential equations. This fact makes the analysis of the system and the design of a control law for it more complicated. Another source

of the nonlinearity of the system under consideration is related to the bounded control resource, $|V| \le \bar{V}$, where $\bar{V}$ is the maximum value of the angular velocity of the actuator driving shaft. Finally, even without the phase and control constraints, the system of equations (5) is not linear because of the presence of trigonometric functions. We are going to reduce it to a linear one by applying the feedback linearization technique. To achieve this goal, we first simplify the system by changing variables.

4 Change of Variables

For the independent variable, we take the path ξ passed by the robot and replace the time derivatives in (5) by the derivatives with respect to ξ. By virtue of the equation $\dot{\xi}(t) = v$, the latter is easily implemented for an arbitrary function $f(t)$ by the evident formula $\dot{f} = vf'$. Here and in what follows, the dot denotes differentiation with respect to time, and the prime without a subscript denotes differentiation with respect to ξ. If a derivative is taken with respect to a different spatial variable, this is explicitly indicated in the subscript (as, e.g., in (1)).

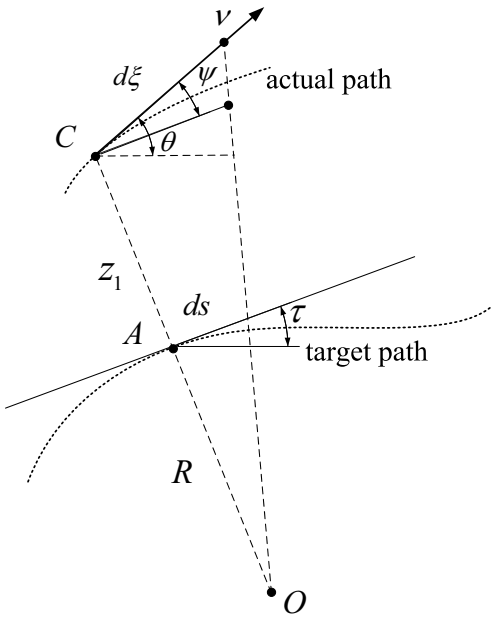

Figure 2. Explanation to change of variables.

Let us introduce some notation explained in Fig. 2. Here, A is the point on the target trajectory that is closest to the current robot position C, and O is the instantaneous center of curvature of the trajectory at the point A, $OA = R(s) \equiv 1/k(s)$. Let τ be the angle between the tangent line to the trajectory at A and the x-axis, and let $\psi = \theta - \tau$. Motion of the vehicle along the target curve in the positive direction is associated with $\psi \approx 0$, whereas $\psi \approx \pi$ corresponds to motion along the curve in the opposite direction.

For the first new phase variable z_1, we take the distance (CA in Fig. 2) from the robot to the target path.[1] From Fig. 2, it is not difficult to see that $\dot{z}_1 = v \sin\psi$. Replacing the time derivative by the derivative with respect to ξ, we obtain

$$z_1' = \frac{\dot{z}_1}{\dot{\xi}} = \sin\psi. \tag{7}$$

For the second phase variable, we take the right-hand side of equation (7), $z_2 = \sin\psi$. Differentiating both sides of this equation with respect to ξ, we get

$$z_2' = \cos\psi \cdot \psi' = \cos\psi \cdot (\theta' - \tau'). \tag{8}$$

The derivative θ' is easily found from (5), $\theta' = \dot{\theta}/\dot{\xi} = u$. The derivative τ' can be found as follows. First, we replace differentiation with respect to ξ by that with respect to the curve parameter s:

$$\tau' = \tau_s' \frac{ds}{d\xi} = k(s)s'. \tag{9}$$

The derivation of the formula for s' is explained in Fig. 2. Indeed, it is not difficult to see that

$$\frac{ds}{d\xi\cos\psi - o(d\xi)} = \frac{R}{R + z_1}.$$

where $o(d\xi)$ is a small quantity with respect to $d\xi$. Hence,

$$s' = \frac{\cos\psi}{1 + kz_1}. \tag{10}$$

Substituting (10) into (9), we obtain

$$\tau' = \frac{k\cos\psi}{1 + kz_1}. \tag{11}$$

Substitution of (11) into (8) yields

$$z_2' = \cos\psi \cdot \left(u - \frac{k\cos\psi}{1 + kz_1}\right). \tag{12}$$

Let us define the third phase variable as

$$z_3 = \cos\psi \cdot \left(u - \frac{k\cos\psi}{1 + kz_1}\right) \tag{13}$$

[1] We do not discuss here the problem of finding the distance to the curve, which may be solved differently for different curves. For example, for a straight line or circular arc, this is a trivial problem. For an arbitrary curve, it can be solved numerically. For B-spline trajectories ([Pesterev, Rapoport, and Gilimyanov, 2007]), the problem is solved by introducing the quasi-distance function, which admits efficient calculation.

and differentiate it with respect to ξ.

Omitting intermediate calculations, which are similar to those above, we obtain

$$z_3' = \pm\sqrt{1-z_2^2}\cdot\left(Lu^2+\frac{1}{L}\right)\cdot\frac{s_{\bar V}(V)}{v} - f(z), \quad (14)$$

where

$$f(z)=\frac{z_2z_3^2}{1-z_2^2}-\frac{kz_2z_3}{1+kz_1}-\frac{k^2z_2(1-z_2^2)}{(1+kz_1)^2}\pm\frac{k_s'(1-z_2^2)^{\frac{3}{2}}}{(1+kz_1)^3}, \quad (15)$$

k_s' is the derivative of the curvature function $k(s)$ and the signs of the first term in (14) and the last term in (15) are the same as that on the right-hand side of the equation

$$\cos\psi = \pm\sqrt{1-z_2^2}. \quad (16)$$

Now, the set of governing equations (5) is rewritten in the z-coordinates as

$$\begin{array}{l} z_1' = z_2, \\ z_2' = z_3, \\ z_3' = \pm\sqrt{1-z_2^2}\left(Lu^2+\frac{1}{L}\right)\frac{V}{v} - f(z), \end{array} \quad (17)$$

where $f(z)$ is given by (15). Note that the old variable u is used here only for convenience of notation. Clearly, u can be expressed in terms of the new variables by means of (13) and (16), and the right-hand of equations (17) is rewritten in terms of only the z-variables.

By virtue of the definition of z_2, we have

$$-1 \le z_2 \le 1. \quad (18)$$

The phase constraints (6) in the new variables take the form

$$-\bar u \le \frac{z_3}{\sqrt{1-z_2^2}} + \frac{k\sqrt{1-z_2^2}}{1+kz_1} \le \bar u. \quad (19)$$

These constraints define the domain of the system under consideration in the z-coordinates.

Constraints (19) hold as equalities when the steering angle is equal to $\pm\alpha_{max}$. The set of all points for which one of constraints (19) holds as the equality is a two-dimensional manifold enclosing the domain of the system. When the system governed by (17) reaches the manifold defined by constraints (19) (α becomes equal to $\pm\alpha_{max}$), the control must be set equal zero (further increase/decrease of the steering angle is impossible). The trajectory of the subsequent motion of the system belongs to the manifold and is governed by the equations

$$\begin{array}{l} z_1' = z_2, \\ z_2' = z_3, \\ z_3' = -\bar f(z), \end{array} \quad (20)$$

where $\bar f(z)$ is the restriction of $f(z)$ to the manifold.

Thus, there does not exist a unique system of equations governing motion of the closed-loop system in the entire domain. In the interior of the domain, the system is governed by equations (17), and on the boundary manifold, by equations (20).

The form of the manifold enclosing the system domain depends on the target trajectory. In Section 6, we consider the simplest case of the target trajectory, where the trajectory is a straight line, and study in detail the manifold and the phase portrait of the system.

5 Control Law Design

Suppose that the point representing the system in the z-coordinates belongs to the interior of the system domain determined by constraints (18)–(19). The choice of control V in (17) in the form

$$V = \pm\frac{v[f(z)-\sigma(z)]}{\sqrt{1-z_2^2}(Lu^2+1/L)}, \quad (21)$$

where the sign on the right-hand side of the equation is selected the same as in the third equation in (17) and σ is a linear function of z given by[2]

$$\sigma = \lambda^3 z_1 + 3\lambda^2 z_2 + 3\lambda z_3,\ \lambda > 0, \quad (22)$$

makes the closed-loop system linear:

$$\begin{array}{l} z_1' = z_2, \\ z_2' = z_3, \\ z_3' = -\sigma. \end{array} \quad (23)$$

This system is equivalent to $z_1''' + 3\lambda z_1'' + 3\lambda^2 z_1' + \lambda^3 z_1 = 0$, which implies the exponential convergence with the rate $-\lambda$ of all components of vector $Z = (z_1, z_2, z_3)^T$.

However, in general, control (21) does not satisfy the two-sided constraints $|V| \le \bar V$, and we should take control in the form

$$V = \pm s_{\bar V}\left(\frac{v[f(z)-\sigma(z)]}{\sqrt{1-z_2^2}(Lu^2+1/L)}\right), \quad (24)$$

[2]Note that it is not necessary to take σ in exactly this form. The particular form of this function determines poles of the closed-loop system. For the given function, the system has one pole $-\lambda$ of multiplicity 3. The other forms of the σ function will imply different poles. The only requirement here is that the poles must have negative real parts.

where $s_{\bar{V}}(V)$ is the saturation function given by

$$s_{\bar{V}}(V) = \begin{cases} -\bar{V} \text{ for } V \le -\bar{V}, \\ V \text{ for } |V| < \bar{V}, \\ \bar{V} \text{ for } V \ge \bar{V}, \end{cases} \tag{25}$$

which, however, does not guarantee exponential decrease of the solution.

When the system reaches the manifold enclosing the system domain, the control is set equal zero, and the subsequent motion of the system is governed by equations (20). At this stage of system motion, the steering angle is fixed, and the trajectories are obtained by mapping the circles of radius R_{min} in the original space into the space of z-coordinates. They belong to the surface (manifold) enclosing the system domain.

The control is turned on again when the right-hand side of (21) changes the sign, which happens when either the function $\bar{f}(z) - \sigma(z)$ or $\cos\psi$ changes its sign. In the former case, the system leaves the manifold and is governed again by equations (23). The latter case takes place when ψ passes through $\pi/2$ or $-\pi/2$ (z_2 reaches 1 or -1, respectively). The analysis of this case is, generally, not specific to the form of the target path and is given in the next section, where the case of the straight target trajectory is discussed. Here, we note only that, in this case, the control switches rapidly between $-\bar{V}$ and $\bar{V}$ (chattering phenomenon), and the system keeps moving on the manifold along the "equator line" $z_2 = 1$ (or $z_2 = -1$), $z_3 = 0$ separating the "top" and "bottom" parts of the manifold (the vehicle approaches the target trajectory in the perpendicular direction with $\psi = \pi/2$ (or $-\pi/2$)). When $\bar{f}(z) - \sigma(z)$ changes sign, the system leaves the equator line and continues moving on the "opposite" part of the manifold (i.e., if α was equal to α_{max}, it turns to $-\alpha_{max}$, and vice versa).

6 Straight Trajectory: Qualitative Analysis

If the target trajectory is a straight line, we have $k(s) = k_s'(s) \equiv 0$, and constraints (19) take the form

$$-\bar{u}\sqrt{1 - z_2^2} \le z_3 \le \bar{u}\sqrt{1 - z_2^2}. \tag{26}$$

Taking constraints (18) into account, we easily find that the domain of the system under consideration is the cylinder with the z_1-axis being the symmetry axis. The cross-section of the cylinder by the plane $z_1 = const$ is the ellipse with the axes directed along the z_2- and z_3-axes; the corresponding semiaxes are equal to 1 and $\bar{u}$, respectively. The function $f(z)$ defined by (15) is simplified for the straight line and given by

$$f(z) = \frac{z_2 z_3^2}{1 - z_2^2}. \tag{27}$$

On the surface of the cylinder, by virtue of (26), $f(z)$ is a linear function:

$$\bar{f}(z) = \bar{u}^2 z_2. \tag{28}$$

It is this function that is used in the third equation in (20).

In this section, to simplify the analysis, we assume that the control V is not bounded and take into account only phase constraints (26). The system "lives" in this cylinder and is governed by equations (23) and (20) in its interior and on the surface (where $|\alpha| = \alpha_{max}$), respectively.

Any trajectory on the surface is an image of a circle of radius R_{min} in the original coordinates to the phase space of the z-coordinates. The projection of this trajectory onto the (z_1, z_2)-plane is the ellipse

$$\bar{u}^2 (z_1 - z_{C1})^2 + z_2^2 = 1, \tag{29}$$

where z_{C1} is the distance from the center of the circle in the original coordinates to the target line, which is easily found by the coordinates of any point belonging to the surface trajectory.

Let us assume that, in the original coordinates, initially, $\cos\psi$ is always positive; i.e., $-\pi/2 \le \psi \le \pi/2$. This assumption implies that the initial orientation of the vehicle agrees with the desired direction of motion along the target line (if $\cos\psi < 0$, the projection of the vehicle velocity on the target line is negative). Then, the right-hand side of equation (21) has the plus sign, and the sign of the control V is determined by the sign of the function $f(z) - \sigma(z)$.

The equation $f(z) - \sigma(z) = 0$ defines a surface passing through the origin; it divides the cylinder into two half-cylinders. In the left half (includes the negative semi-axis z_1), the function is positive, and, in the right half (includes the positive semi-axis z_1), negative. On the surface of the cylinder, the equation $f(z) - \sigma(z) = 0$ defines a *switching line,* the curve separating the cylinder surface into two—"positive" and "negative"—parts. By virtue of (28), this curve is an ellipse obtained by the intersection of the cylinder surface and the plane

$$\bar{u}^2 z_2 - \lambda^3 z_1 - 3\lambda^2 z_2 - 3\lambda z_3 = 0. \tag{30}$$

Figure 3 shows the top view of the "phase cylinder." The oblong ellipse in the center of the cylinder shows the switching line for a vehicle model with $\bar{u} = 0.236$ ($R_{min} \approx 4.24$ m) for $\lambda = 1$. The solid line is the visible part of this line on the top cylinder surface, the invisible part of the line on the bottom surface is depicted by the dashed line. The other two elliptic trajectories girding the cylinder are solutions to equations (20) corresponding to different initial conditions; the equations of the projection of these 3D curves on the

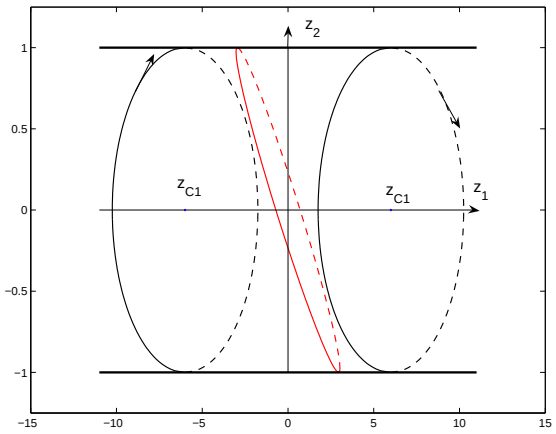

Figure 3. Top view of system domain.

(z_1, z_2)-plane are given by (29). The solid and dashed lines correspond to the fragments of these curves on the top and bottom surfaces, respectively. The arrows show the direction of motion. Any trajectory on the surface is obtained from another by simply shifting it along the z_1-axis.

Consider an arbitrary point in the cylinder representing an initial position of the vehicle. Let, for definiteness, it be located in the left half-cylinder. Then, V is positive, the angle α increases, and the representing point moves toward the top surface. Note that the system cannot appear on the bottom surface of the left half-cylinder. Further, we have two possibilities. First, if the steering angle does not reach its maximum value, the trajectory lies in the interior of the cylinder and converges exponentially to the origin, which corresponds to stabilization of motion along the target line. This case takes place if the initial position is close enough to the origin or/and λ is relatively small. In the general case, however, the trajectory reaches the upper surface of the cylinder. At this point, the control must be set equal zero, and the subsequent motion of the system is governed by the system of equations (20). The system moves along one of the surface trajectories similar to the left trajectory in Fig. 3. Consider two possible cases of mutual location of this trajectory and the switching line, namely, the cases where, on the top surface, these curves (1) intersect and (2) do not intersect (as in Fig. 3).

In the former case, the control V given by (21) changes the sign at the intersection point, and the angle α starts to diminish. Hence, the system leaves the surface and goes inside the cylinder. Further, it can either stay inside the cylinder and converge exponentially to the origin or come down the bottom surface and start to move along one of the trajectories similar to the right ellipse in Fig. 3.

In the latter case, we have the following picture. When the surface trajectory intersects the equator line $z_2 = 1$, the right-hand side of (21) changes the sign (due to $\cos\psi$), and the control turns on. Since the control is very large (when ψ passes through the angle $\pi/2$, the right-hand side of (21) jumps from $+\infty$ to $-\infty$), the steering angle rapidly diminishes and reaches its minimum value $-\alpha_{max}$; the angle ψ starts to decrease and becomes again less than $\pi/2$. As a result, the control V changes the sign again, and so on. Hence, we have chattering, when the control switches from large negative values to positive ones, and vice versa; the steering angle also rapidly varies between $-\alpha_{max}$ and $+\alpha_{max}$, and the vehicle moves along the line perpendicular to the target line with $\psi = \pi/2$. In the z-coordinates, the representing point does not leave the surface and moves along the equator line. Thus, we arrive at the following proposition.

Proposition. No matter how far the initial point from the target line, the system will necessarily come in the vicinity of the line.

Indeed, the above reasoning shows that, starting from an arbitrary initial point, the system will come up (down) the top (bottom) surface; then, if the point is far from the line, will reach the equator line; and, moving along this line, will reach the switching line. The distance from the intersection point to the target line depends on λ and is easily found by substituting $z_2 = \pm 1$ and $z_3 = 0$ into (30) resulting in $|z_1| = (3\lambda^2 - \bar{u}^2)/\lambda^3$.

Then, given that the system came to the equator line from the top surface, after intersecting the switching line, it starts moving along an elliptic trajectory on the bottom surface with $\alpha = -\alpha_{max}$. It can easily be seen from the figure (see also Fig. 4) that the point of intersection of the latter trajectory with the switching line is closer to the origin ($|z_2| < 1$ and $|z_1|$ is less than that of the previous intersection point). Note that the motion of the system on the top surface of the right half-cylinder is impossible.

Moreover, our analysis and numerical experiments make us assume that, if the system trajectory intersects the switching line, then the system will necessarily converge to the origin (i.e., the system stabilizes along the target line). This assumption is based on the observation that the subsequent points of the intersection of a trajectory approach the origin (see numerical example below). However, it has not been strictly proved yet.

7 Numerical Example

To illustrate the above said, we modeled the controlled motion of a vehicle with $\alpha_{max} = \pi/6$ and $L = 2.45$ m ($\bar{u} = 0.236$) moving with a speed $v = 2$ m/s located initially at the distance of 7 m from the target line with $\theta = 0$ ($z_1 = -7$, $z_2 = 0$, and $z_3 = 0$). The value of λ in the control law (21) was set equal to 1.5. Figure 4 shows the projection of the phase trajectory onto the (z_1, z_2)-plane. The dots on the trajectory show the points of intersection of the trajectory with the equator and switching lines and the points where the trajectory comes up (down) the surface. The fragments of the trajectories lying on the top surface are depicted by the solid lines, and those on the bottom surface or inside

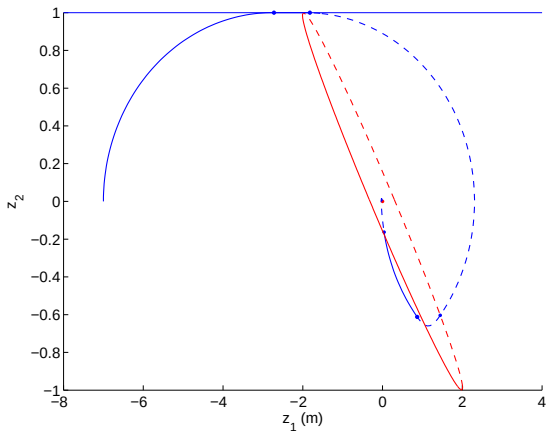

Figure 4. Projection of the phase trajectory onto the (z_1, z_2)-plane.

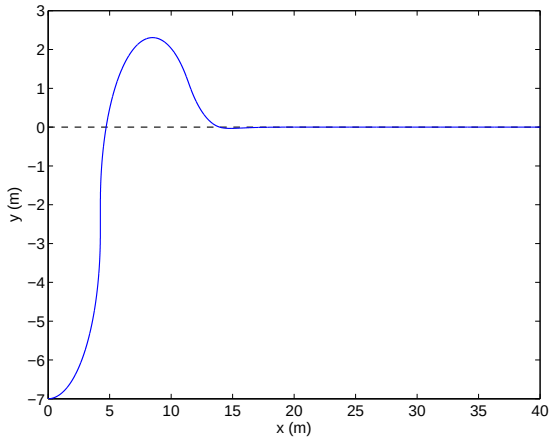

Figure 5. Target straight path (dashed line) and actual trajectory (solid line).

the cylinder, by the dashed lines.

As can be seen, the trajectory rapidly reaches the top surface and consists of six segments (separated by dots). The first segment belongs to the top surface and corresponds to the circular motion with $\alpha = \alpha_{max}$. Next, the vehicle moves perpendicular to the target line (along the equator line in the z-coordinates). After passing the switching line, the steering angle turns to $-\alpha_{max}$, and the vehicle moves on the bottom surface (the third segment). After passing the switching line, in the fourth segment, the vehicle moves inside the cylinder until it comes up the top surface. The fifth segment—motion on the top surface with $\alpha = \alpha_{max}$—is short and ends up after intersection of the switching line. The last, sixth, segment belongs to the interior of the cylinder and terminates at the origin.

The corresponding physical trajectory in the original (x, y) coordinates is shown in Fig. 5. The target straight path is depicted by the dashed line.

8 Conclusions

The control problem for a mobile robot with regard to the actuator dynamics has been considered. By applying change of variables, the system is reduced to the form for which the equilibrium stability problem can be set. For this system, a control law has been synthesized with regard to phase constraints and constraints on control. For a straight target path, qualitative analysis of the system is given, and phase trajectories are studied. Results of numerical modeling are presented.

Acknowledgements

This work was supported by the Presidium of Russian Academy of Sciences (Program 22) and by the state program of support of leading scientific schools (project no. NSh-1676.2008.1).

References

Cordesses, L., Cariou, C., and Berducat, M. (2000) Combine Harvester Control Using Real Time Kinematic GPS. *Precision Agriculture*, **2**, pp. 147–161.

Thuilot, B., Cariou, C., Martinet, P., and Berducat M. (2002) Automatic Guidance of a Farm Tractor Relying on a Single CP-DGPS. *Autonomous Robots*, **15**, pp. 53–61.

Rapoport, L.B., et al. (2006) Control of Wheeled Robots Using GNSS and Inertial Navigation: Control Law Synthesis and Experimental Results. *Proc. ION GNSS 2006, The 19th International Technical Meeting*, Long Beach, USA, pp. 2214–2221.

Samson. C. (1995) Control of Chained Systems Application to Path Following and Time-Varying Point-Stabilization of Mobile Robots. *IEEE Trans. Automat. Control*, **40**, pp. 64–77.

Kolmanovsky, I. and McClamroch, N.H. (1995) Developments in Nonholonomic Control Problems. *IEEE Control Systems Magazine*, **15**, pp. 20–36.

Guldner, J. and Utkin, V.I. (1994) Stabilization of nonholonomic mobile robots using Lyapunov functions for navigation and sliding mode control. *Proc. 33rd IEEE Conf. Decision Control*, pp. 2967–2972.

Rapoport L.B. (2006) Estimation of Attraction Domains in Wheeled Robot Control, *Automation and Remote Control* 67:pp. 1416–1435.

Pesterev A.V., Rapoport L.B., and Gilimyanov R.F. (2007) Global Energy Fairing of B-Spline Curves in Path Planning Problems. *Proc. of the ASME 2007 IDETC*, Las Vegas, CD ROM.